Reduction-Based Control of Branched Chains: Application to Three-Dimensional Bipedal Torso Robots

Robert D. Gregg and Mark W. Spong

Abstract— **This paper revisits the concept of controlled reduction, a symmetry-based method of decomposing the control of mechanical systems into lower-dimensional problems. Founded on a geometric property of serial kinematic chains termed *recursive cyclicity*, the present work extends this property to branched chains by defining the minimal *irreducible tree structure*. We then generalize the *Subrobot Theorem* to branched chains, showing that we can use control to reduce any robot's dimensionality to that of its irreducible tree structure. This method is applied to a 5-DOF bipedal robot with a hip and torso – we construct stable straight-ahead and turning gaits in 3-D space based on known sagittal-plane limit cycles.**

I. Introduction

Humanoid walking has become an active area of research in the robotics community over the past decades. Researchers believe robotic devices will soon prove essential in rehabilitation, prosthesis, and assisted locomotion. The incredible efficiency of bipedal walking motivates its use on locomotive mechanisms. However, robotic imitation has had limited success in simultaneously addressing three important humanoid traits: the motion is dynamic, involving pendular falling towards the ground; three-dimensional, involving three planes-of-motion; and complex, involving a branching tree structure with many coupled degrees-of-freedom (DOF).

Early work on dynamic walking began with simple serial-chain models constrained to the sagittal plane (2-D space), such as the uncontrolled two-link "compass-gait" biped, to roughly approximate human dynamic motion. In the pioneering work of [14], McGeer discovered the existence of stable "passive" limit cycles down shallow slopes between about 3° and 5°. Gravity-powered passive walking was further studied in [7] and extended to spatially 3-D bipeds (pitch and lean without yaw) by controlling leg splay in [12].

More anthropomorphic forms of the compass-gait biped have also been adopted. Grizzle et. al. proved that asymptotically stable limit cycles can be generated for planar walkers, such as the compass-gait-with-torso biped, using the concept of hybrid zero dynamics [21], based on output linearization about hybrid-invariant virtual constraints describing the walking gait. This underactuated control method was recently generalized to spatially and completely 3-D torso bipeds in [4], [16]. In unrelated work, Collins built a biped with arms that demonstrated 3-D passive walking [5], after being carefully tuned to walk straight down a fixed slope.

Passive dynamics were embraced in the active feedback methods of passivity-based control and controlled symmetries [18]–[20], showing that passive limit cycles down slopes could be mapped to "pseudo-passive" limit cycles on arbitrary slopes with expanded basins of attraction. This requires the existence of stable passive limit cycles, which is usually not the case for complex 3-D bipeds, so the primary application of this method has been sagittal-plane walking.

However, these geometric methods remained appealing due to the natural and efficient dynamic gaits they produced for planar robots. Ames et al. suggested the use of a controlled form of symmetry-based reduction to decompose a spatially 3-D biped's dynamics into the sagittal plane-of-motion, which is well understood, and a separate lean mode in the frontal (or lateral) plane [2], [3]. The present authors generalized this method to controlled reduction by stages in [10], so as to separate the yaw and lean dynamics from a completely 3-D hipped biped. The resulting sagittal subsystem had the dynamics of an associated planar biped, from which asymptotically stable full-order walking gaits were built about arbitrary headings.

This was shown to be applicable to all serial kinematic chains in [10], by identifying extensive symmetries with the *recursively cyclic* property of inertia matrices. We then introduced the *Subrobot Theorem*, showing that reduction-based control can decompose any serial chain for lower-dimensional analysis. In the robotic walking context, this simplified the search for full-order limit cycles and expanded the class of 3-D bipeds that can achieve pseudo-passive dynamic walking. However, this class was limited to serial kinematic chains, preventing application to bipeds with branching torsos and arms.

This paper extends controlled reduction to the general class of open kinematic chains. In particular, we show that branched chains can be mapped to our familiar serial-chain framework, allowing us to prove certain symmetries needed for reduction. We demonstrate this on a 5-DOF biped with a hip and torso, presenting a reduction-based control law that imposes a 2-stage controlled reduction to the robot's stabilized sagittal-plane subsystem. This also provides momentum control to force the biped's lean to vertical and yaw to the desired heading angle between steps. We use this controller to build both straight-ahead and turning gaits on flat ground, which are 2-periodic (modulo heading change) due to natural side-to-side swaying motion induced by the robot's hip. This nicely resembles the discussed traits of humanoid walking.

R. D. Gregg is with the Department of Electrical and Computer Engineering, University of Illinois at Urbana-Champaign, Urbana, IL 61801 rgregg@illinois.edu http://decision.csl.uiuc.edu/∼rgregg/

M. W. Spong is with the Department of Electrical Engineering, University of Texas at Dallas, Richardson, TX 75080 mspong@utdallas.edu

This research was partially supported by NSF Grant CMS-0510119.

II. Dynamics and Symmetry

In order to identify the symmetries needed for reduction, we first describe a robot's typical Lagrangian dynamics.

Lagrangian Dynamics. A mechanical system with configuration space Q is described by elements $(q, \dot{q})$ of tangent bundle[1] TQ and the Lagrangian function $L : TQ \to \mathbb{R}$, given in coordinates by

$$L(q, \dot{q}) = K(q, \dot{q}) - V(q) = \frac{1}{2}\dot{q}^T M(q)\dot{q} - V(q),$$

where $K(q, \dot{q})$ is the kinetic energy, $V(q)$ is the potential energy, and $M(q)$ is the $n \times n$ symmetric, positive-definite inertia matrix. By the least action principle [13], L satisfies the n-dimensional controlled Euler-Lagrange (E-L) equations

$$\frac{d}{dt}\frac{\partial L}{\partial \dot{q}} - \frac{\partial L}{\partial q} = Bu,$$

the dynamics for the controlled robot are given by

$$M(q)\ddot{q} + C(q, \dot{q})\dot{q} + N(q) = Bu,$$

where $n \times n$-matrix $C(q, \dot{q})$ contains the Coriolis/centrifugal terms, $N(q) = \frac{\partial}{\partial q}V(q)$ is the vector of potential torques, $n \times n$-matrix B is assumed invertible for full actuation, and control input u is an n-vector of joint actuator torques.

These equations yield the dynamical control system (f, g):

$$\begin{pmatrix} \dot{q} \\ \ddot{q} \end{pmatrix} = f(q, \dot{q}) + g(q)u, \tag{1}$$

with vector field f and matrix g of control vector fields:

$$\begin{aligned} f(q, \dot{q}) &= \begin{pmatrix} \dot{q} \\ M(q)^{-1}\left(-C(q, \dot{q})\dot{q} - N(q)\right) \end{pmatrix} \\ g(q) &= \begin{pmatrix} 0_{n\times n} \\ M(q)^{-1}B \end{pmatrix}. \end{aligned}$$

If L has certain symmetries, i.e., invariance under the action of a symmetry group on Q, we can simplify these dynamics.

Symmetries and Reduction. Geometric reduction is an analytical method of decomposing the dynamics of a system with symmetries. A few forms of reduction are discussed in [13], such as Lie-Poisson, Euler-Poincaré, and Routh.

In the classical form of *Routhian reduction*, Lagrangian L has configuration space $Q = \mathbb{G} \times S$ (in our case, an n-torus), where $\mathbb{G} = \mathbb{G}_1 \times \ldots \times \mathbb{G}_k$ is the *symmetry group* and $S \cong Q \backslash \mathbb{G}$ is the *shape space*. Symmetries of L are characterized by *cyclic* variables $q_i \in \mathbb{G}_i$, such that

$$\frac{\partial L}{\partial q_i} = 0, \quad i \in \{1, k\}. \tag{2}$$

Hence, L is invariant under the action of rotating such coordinates. Equation (2) implies that the generalized momentum of each cyclic coordinate is constant. The dynamics then evolve on level-sets of these conserved momentum constraints, where we can directly relate solution curves of the full-order system on phase space TQ to solution curves of a reduced-order system on phase space TS, and vice versa.

[1]Tangent bundle TQ: space of configurations and their tangent velocities.

In other words, we divide out group $\mathbb{G}$ by projecting TQ onto reduced space $TS \cong TQ \mod T\mathbb{G}$. However, stability in TS says nothing about the stability of the divided coordinates (which in the context of walking are the unstable yaw and lean modes). The controlled form of geometric reduction, *functional Routhian reduction*, breaks the symmetry of group $\mathbb{G}$ to provide momentum control of its coordinates [2], [3], [10]. We will show that symmetry-breaking is imposed in a specific manner so that the group $\mathbb{G}$ of "almost-cyclic" variables can still be divided.

III. Controlled Reduction by Stages

In this section, we present the k-stage case of controlled reduction for an n-DOF robot, $1 \leq k < n$, based on the single-stage construction of [3]. In order to control the divided variables, we define a special class of Lagrangians that have "almost-cyclic" variables.

k-Almost-Cyclic Lagrangians. We start with a general n-dim. configuration space $Q = \mathbb{T}^k \times S$, where shape space $S \cong Q \backslash \mathbb{T}^k$ is constructed by $n - k$ copies of $\mathbb{R}$ and circle $\mathbb{S}^1$, and $\mathbb{T}^k = \mathbb{S}^1 \times \ldots \times \mathbb{S}^1$ is the group of "almost-cyclic" variables to be divided in stages of $\mathbb{S}^1$. We denote a configuration $q = (q_1, \ldots, q_n)^T = (q_1^{i^T}, q_{i+1}^{n^T})^T \in Q$ for $1 \leq i \leq n$, with i-dim. vector q_1^i containing coordinates $q_1, \ldots, q_i$ and $(n-i)$-dim. vector q_{i+1}^n containing $q_{i+1}, \ldots, q_n$ (clearly, if $i = n$ then $q_{n+1}^n = \emptyset$). In particular, for $i = k$ we have the vector of almost-cyclic variables $q_1^k \in \mathbb{T}^k$ and the vector of shape space variables $q_{k+1}^n \in S$. To begin, let inertia matrix M be defined from a class of *recursively cyclic* matrices, giving us the symmetries we need for reduction.

Definition 1: An $n \times n$-matrix M is *recursively cyclic* if each lower-right $(n-i+1)\times(n-i+1)$ submatrix is cyclic in $q_1, \ldots, q_i$ for $1 \leq i \leq n$, i.e., it has the form of (3) with base case $i = n$, where $M_{q_n^n}(q_{n+1}^n) = m_{q_n}$ is a scalar constant.

Remark 1: In our case, for $1 \leq i \leq n$, each $m_{q_i}(\cdot)$ is the scalar positive-definite self-induced inertia term of coordinate q_i, and $M_{q_i, q_{i+1}^n}(\cdot) \in \mathbb{R}^{i-1}$ is the row vector of off-diagonal inertial coupling terms between q_i and coordinates q_{i+1}^n. Moreover, $M_{q_i^n}(\cdot) \in \mathbb{R}^{(n-i+1)\times(n-i+1)}$ is the symmetric positive-definite inertia submatrix of coordinates q_i^n.

A special class of shaped Lagrangians termed *almost-cyclic Lagrangians* is defined in [3], allowing one stage of controlled reduction to a subsystem characterized by a *functional Routhian* – the Lagrangian function of the lower-dim. system. In order to control k divided variables, each stage of reduction must project from an almost-cyclic Lagrangian (ACL) to another ACL for the next stage of reduction, until the final stage reaches the base functional Routhian. Therefore, we are interested in a generalized ACL.

Definition 2: A Lagrangian $L_{\lambda_1^k} : T\mathbb{T}^k \times TS \to \mathbb{R}$ is *k-almost-cyclic* if, in coordinates, it has the form

$$L_{\lambda_1^k}(q, \dot{q}) = K_{\lambda_1^k}(q, \dot{q}) - V_{\lambda_1^k}(q)$$

with expanded terms given in (4)-(6) for $j = 1$ and some arbitrary functions $\lambda_i : \mathbb{S}^1 \to \mathbb{R}$, $i \in \{1, k\}$.

$$M(q_2^n) = \begin{pmatrix} m_{q_1}(q_2^n) & M_{q_1,q_2^n}(q_2^n) \\ M^T_{q_1,q_2^n}(q_2^n) & M_{q_2^n}(q_3^n) \end{pmatrix} = \begin{pmatrix} m_{q_1}(q_2^n) & \text{—} & M_{q_1,q_2^n}(q_2^n) & \text{——} \\ | & \ddots & & \vdots \\ M^T_{q_1,q_2^n}(q_2^n) & & m_{q_{i-1}}(q_i^n) & M_{q_{i-1},q_i^n}(q_i^n) \\ | & \cdots & M^T_{q_{i-1},q_i^n}(q_i^n) & M_{q_i^n}(q_{i+1}^n) \end{pmatrix} \tag{3}$$

$$L_{\lambda_j^k}(q_j^n, \dot{q}_j^n) = K_{\lambda_j^k}(q_j^n, \dot{q}_j^n) - V_{\lambda_j^k}(q_j^n) = \frac{1}{2}\dot{q}_j^{n\,T} M_{\lambda_j^k}(q_{j+1}^n)\dot{q}_j^n - W_{\lambda_j^k}(q_j^n, \dot{q}_{j+1}^n) - V_{\lambda_j^k}(q_j^n) \tag{4a}$$

$$\begin{aligned} &= L_{\lambda_{j+1}^k}(q_{j+1}^n, \dot{q}_{j+1}^n) + \frac{1}{2} m_{q_j}(q_{j+1}^n)(\dot{q}_j)^2 + \dot{q}_j M_{q_j,q_{j+1}^n}(q_{j+1}^n)\dot{q}_{j+1}^n \\ &\quad + \frac{1}{2}\dot{q}_{j+1}^{n\,T} \frac{M^T_{q_j,q_{j+1}^n}(q_{j+1}^n) M_{q_j,q_{j+1}^n}(q_{j+1}^n)}{m_{q_j}(q_{j+1}^n)} \dot{q}_{j+1}^n - \frac{\lambda_j(q_j)}{m_{q_j}(q_{j+1}^n)} M_{q_j,q_{j+1}^n}(q_{j+1}^n)\dot{q}_{j+1}^n + \frac{1}{2}\frac{\lambda_j(q_j)^2}{m_{q_j}(q_{j+1}^n)} \end{aligned} \tag{4b}$$

$$M_{\lambda_j^k}(q_{j+1}^n) = M_{q_j^n}(q_{j+1}^n) + \sum_{i=j}^{k} \begin{pmatrix} 0_{i\times i} & 0_{i\times(n-i)} \\ 0_{(n-i)\times i} & \frac{M^T_{q_i,q_{i+1}^n}(q_{i+1}^n) M_{q_i,q_{i+1}^n}(q_{i+1}^n)}{m_{q_i}(q_{i+1}^n)} \end{pmatrix} \tag{5}$$

$$W_{\lambda_j^k}(q_j^n, \dot{q}_{j+1}^n) = \sum_{i=j}^{k} \frac{\lambda_i(q_i)}{m_{q_i}(q_{i+1}^n)} M_{q_i,q_{i+1}^n}(q_{i+1}^n)\dot{q}_{i+1}^n, \qquad V_{\lambda_j^k}(q_j^n) = V_{\text{fct}}(q_{k+1}^n) - \frac{1}{2}\sum_{i=j}^{k} \frac{\lambda_i(q_i)^2}{m_{q_i}(q_{i+1}^n)} \tag{6}$$

Remark 2: The closed-form definition (4a) explicitly shows all the shaping terms necessary for k stages of controlled reduction, whereas the last three terms in recursive definition (4b) impose a single stage of controlled reduction to $(k-1)$-almost-cyclic Lagrangian $L_{\lambda_2^k}$.

Given k-almost-cyclic Lagrangian (k-ACL) $L_{\lambda_1^k}$, the n-dimensional fully-actuated E-L equations yield

$$M_{\lambda_1^k}(q_2^n)\ddot{q} + C_{\lambda_1^k}(q, \dot{q})\dot{q} + N_{\lambda_1^k}(q) = Bv. \tag{7}$$

Then, we have the control system on TQ associated with $L_{\lambda_1^k}$ as defined in (1): $(f_{\lambda_1^k}, g_{\lambda_1^k})$ with control input v.

This input can be decomposed into v_1^k, the vector containing the first k elements, and v_{k+1}^n, the $(n-k)$-vector containing elements $k+1, \ldots, n$. Assuming subsystem input v_{k+1}^n is defined by a time-invariant feedback control law on TS, we incorporate this into the full-order k-ACL system by defining the new control system $(\hat{f}_{\lambda_1^k}, \hat{g}_{\lambda_1^k})$ with input v_1^k:

$$\begin{aligned} \hat{f}_{\lambda_1^k}(q, \dot{q}) &:= f_{\lambda_1^k}(q, \dot{q}) + g_{\lambda_1^k}(q) \begin{pmatrix} 0_{k\times 1} \\ v_{k+1}^n \end{pmatrix} \\ \hat{g}_{\lambda_1^k}(q) &:= g_{\lambda_1^k}(q) \begin{pmatrix} I_{k\times k} \\ 0_{(n-k)\times k} \end{pmatrix}. \end{aligned} \tag{8}$$

Here, vector field $\hat{f}_{\lambda_1^k}$ corresponds to the v_{k+1}^n-controlled E-L equations, which will be relevant later.

Reduced Subsystems. Starting with this k-ACL system, each reduction stage projects onto a lower-dimensional system while conserving a momentum quantity corresponding to the divided degree-of-freedom. These coordinates can thus be uniquely reconstructed by the functional momentum maps $J_i : T(Q\backslash\mathbb{T}^{i-1}) \to \mathbb{R}$, $i \in \{1, k\}$:

$$\begin{aligned} J_i(q_i^n, \dot{q}_i^n) &= \frac{\partial}{\partial \dot{q}_i} L_{\lambda_i^k}(q_i^n, \dot{q}_i^n) \\ &= M_{q_i,q_{i+1}^n}(q_{i+1}^n)\dot{q}_{i+1}^n + m_{q_i}(q_{i+1}^n)\dot{q}_i \\ &= \lambda_i(q_i). \end{aligned} \tag{9}$$

Here, $L_{\lambda_i^k}$ is the k-ACL for $i = 1$ or a lower-dim. ACL for $i \in \{2, k\}$. In classical Routh reduction, each J_i maps to a constant momentum quantity. However, the energy shaping terms in $L_{\lambda_1^k}$ break these conservative maps and force them equal to desirable functions $\lambda_i(q_i)$. Hence, we can control the momenta of the divided coordinates.

Each of these reduced subsystems is characterized by a generalized functional Routhian. For $j \in \{2, k\}$, the Routhian function corresponding to the $(j-1)^{\text{st}}$ stage of reduction is a $(k-j+1)$-ACL on the tangent bundle of reduced configuration space $Q\backslash\mathbb{T}^{j-1}$. This is the *stage-$(j-1)$ functional Routhian* $L_{\lambda_j^k} : T(Q\backslash\mathbb{T}^{j-1}) \to \mathbb{R}$, obtained through a partial Legendre transformation in q_{j-1} constrained to functional momentum map (9) for $i = j-1$:

$$\begin{aligned} L_{\lambda_j^k}(q_j^n, \dot{q}_j^n) &= L_{\lambda_{j-1}^k}(q_{j-1}^n, \dot{q}_{j-1}^n) - \lambda_{j-1}(q_{j-1})\dot{q}_{j-1}\Big|_{J_{j-1}} \\ &= K_{\lambda_j^k}(q_j^n, \dot{q}_j^n) - V_{\lambda_j^k}(q_j^n). \end{aligned}$$

We see that for $j \in \{2, k\}$, $L_{\lambda_j^k}$ has the form of (4).

The final stage of reduction, stage-k, is a functional Routhian $L_{\lambda_{k+1}^k} = L_{\text{fct}}$ with a traditional Lagrangian structure. This is similarly obtained from stage-$(k-1)$ functional Routhian $L_{\lambda_k^k}$. It follows that the k-reduced Lagrangian $L_{\text{fct}} : TS \to \mathbb{R}$ is given in coordinates by

$$L_{\text{fct}}(q_{k+1}^n, \dot{q}_{k+1}^n) = \frac{1}{2}\dot{q}_{k+1}^{n\,T} M_{q_{k+1}^n}(q_{k+1}^n)\dot{q}_{k+1}^n - V_{\text{fct}}(q_{k+1}^n)$$

with target potential energy V_{fct}.

This yields the control system on TS associated with L_{fct}: $(f_{\text{fct}}, g_{\text{fct}})$ with input v_{k+1}^n. From this, we define the vector field corresponding to the k-reduced, controlled dynamics:

$$\hat{f}_{\text{fct}}(q_{k+1}^n, \dot{q}_{k+1}^n) := f_{\text{fct}}(q_{k+1}^n, \dot{q}_{k+1}^n) + g_{\text{fct}}(q_{k+1}^n)v_{k+1}^n. \tag{10}$$

When $v_1^k = 0$ and the functional momentum quantities abide by (9), there exists a map between solutions of full-order vector field $\hat{f}_{\lambda_1^k}$ and reduced-order vector field $\hat{f}_{\text{fct}}$.

Theorem 1: Let $L_{\lambda_1^k}$ be a k-ACL with stage-k functional Routhian $L_{\rm fct}$. Then, $\left(q_1^k(t), q_{k+1}^n(t), \dot{q}_1^k(t), \dot{q}_{k+1}^n(t)\right)$ is a solution to v_{k+1}^n-controlled vector field $\hat{f}_{\lambda_1^k}$ on $[t_0, t_f]$ with

$$J_j(q_j(t_0), \dot{q}_j(t_0)) = \lambda_j(q_j(t_0)), \ \forall \ j \in \{1, k\},$$

if and only if $(q_{k+1}^n(t), \dot{q}_{k+1}^n(t))$ is a solution to controlled vector field $\hat{f}_{\rm fct}$ on $[t_0, t_f]$ and $(q_j(t), \dot{q}_j(t))$ satisfies

$$J_j(q_j(t), \dot{q}_j(t)) = \lambda_j(q_j(t)), \ \forall \ j \in \{1, k\}, \ \text{on} \ [t_0, t_f].$$

Note that (9) can be solved for $\dot{q}_j$ to reconstruct each coordinate. We want to apply this form of controlled reduction, proven in [10], to general robots, but we certainly cannot expect robots to naturally be k-almost-cyclic. It is shown in [10] that serial kinematic chains can attain the special k-almost-cyclic form through energy-shaping control. We wish to show that there also exists such a class of "reduction-based" controllers for more general branched chains.

IV. Exploiting Symmetries in Branched Chains

The primary theoretical contribution of this paper is extending controlled reduction and the Subrobot Theorem to branched chains. In order to do this, we first discuss how to model branched chains in a familiar framework.

Mapping Branched Chains to Serial Chains. A popular theory for modeling multibody systems with tree structure is presented in [22]. Such systems have a uniquely defined path between any two bodies (and are composed of nested tree substructures). A branched chain can then be characterized by a directed graph of vertices and arcs originating from a carrier/base body. Dynamics of each body are derived based on the path from the base vertex to the vertex of the concerned body. This is employed in [1] for simulating multilegged robots, where the authors suggest that geometric reduction might be useful for controlling such complex systems. We do just this, but we investigate symmetries using a different modeling approach.

In order to apply controlled reduction as presented, we model a branched chain as a single higher-order *redundant serial chain* that essentially wraps around each branch (i.e., each radiating serial chain). Here, it is intuitive to describe each DOF as a vertex to be reduced from the directed graph, so we represent each interconnection as a vertex and each link/body as an arc, labeled in increasing order from the base vertex. An interconnection can be either a joint (one- to three-DOF) or a fixed-angle connection between links.

A branch is characterized by a directed path to the branch tip, along with a *redundant path* returning to the base of that branch (except for the branch that concludes the redundant serial chain, see Fig. 1). A redundant path is composed of zero-mass/inertia *redundant links* and *redundant interconnections*, always constrained as a fixed-angle connection (at the end of a branch) or a joint constrained to mirror a previous joint along the branch. In the example of Fig. 1, the first branch is a *simple branch*, since it only has a fixed-angle redundancy $i_2^r = \pi$, whereas the second branch has variable constraints $i_4^r = i_5$, $i_5^r = i_6$ along with

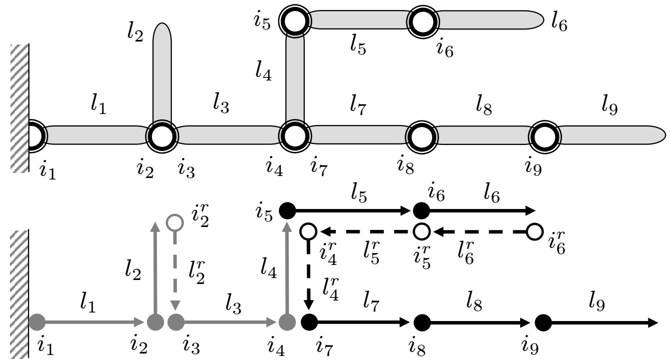

Fig. 1. A branched chain modeled as a serial chain in a directed graph. The reducible part is in grey and the irreducible tree structure in black.

fixed $i_6^r = \pi$. Due to these trivial constraints, the higher-order redundant chain is described by a differential-algebraic system of equations, which can be trivially projected onto n-DOF constrained dynamics [15], by grouping like terms. The redundant dynamics evolve on this invariant constrained manifold, so solutions exist uniquely and are equivalent to branched-chain solutions by construction.

Subrobot Theorem. We can now revisit the Subrobot Theorem of [10], which shows that any fully actuated serial-chain robot can be controlled as a lower-dimensional subsystem. To begin, we state the geometric property of recursive cyclicity, which is the basis behind the result that follows.

Lemma 1: The inertia matrix of any serial kinematic chain is recursively cyclic as in Definition 1.

Lemma 2: For any fully-actuated n-DOF serial-chain robot with a potential energy that is cyclic in the first k coordinates, $1 \leq k < n$, there exists a feedback control law that shapes the system to the k-almost-cyclic form.

Hence, after controlled reduction by Theorem 1, dynamical analysis can be restricted to the behavior of the $(n-k)$-DOF subrobot down the chain. Generalizing this result to the branching case is not trivial – recursive cyclicity does not always hold for the inertia matrix of a branched chain. This is because redundant joints of a non-simple branch are constrained equal to previous angles along the branch. For example, in Fig. 1 we saw that $i_4^r = i_5$, and this constraint's right-hand-side is a coordinate from earlier in the chain. This introduces an inherently non-cyclic dependence on i_5 in the inertia submatrix associated with the coordinates from i_5 to the end of the chain. The necessary symmetries do not exist to reduce this part of the branched chain in the framework of Theorem 1. However, we should not give up yet – there are symmetries in the chain prior to this troubling branch that can be exploited. To formalize this notion, we define the irreducible tree structure of a branched chain.

Definition 3: The *irreducible tree structure* of an n-DOF branched chain is the minimal m-DOF tree substructure, $1 \leq m \leq n$, at the end of the chain such that the corresponding inertia submatrix is not recursively cyclic.

This definition has two trivial cases. Case $m = 1$ occurs when the entire chain is controlled-reducible, such as with serial chains by Lemma 2. We will not consider the opposite case $m = n$, when two or more non-simple chains branch directly from the carrier body, since these are best modeled as separate, decoupled serial chains. In general, any branched chain with only simple branches is entirely reducible, since all redundant joints are fixed angles and introduce no dependencies on previous angles to violate recursive cyclicity. This fact also gives us the following:

Proposition 1: The inertia matrix of any branched chain is recursively cyclic down to the second joint of the first non-simple branch. I.e., the submatrix corresponding to the remaining part of the redundant serial chain is irreducible.

This is proven by applying Lemma 1 to the redundant serial chain until we reach the second joint of a non-simple branch, which has a variable constraint at the corresponding redundant interconnection (the base joint of such a branch does not affect the configuration of other branches from that base). For example, the irreducible tree structure of the branched chain in Fig. 1 is shown in black. We can now introduce the branching Subrobot Theorem.

Lemma 3: For any fully actuated n-DOF branched-chain robot with an m-DOF irreducible tree structure, $1 \leq m < n$, and a potential energy that is cyclic in the first k coordinates, $1 \leq k \leq (n - m)$, there exists a feedback control law that shapes the system to the k-almost-cyclic form.

Theorem 2: Suppose an n-DOF branched-chain robot has an m-DOF irreducible tree structure, $1 \leq m < n$, and a potential energy that is cyclic in the first k coordinates, $1 \leq k \leq (n-m)$. Then, the n-DOF robot is controlled-reducible down to its corresponding $(n - k)$-DOF subrobot.

Remark 3: Even if a robot's potential energy does not have the necessary symmetries, we can use potential shaping control to eliminate dependencies on the variables we wish to reduce, i.e., we impose a "controlled symmetry" to satisfy the assumptions of Lemma 3. Therefore, we can impose a controlled reduction down to the m-DOF irreducible tree structure, which is trivially the last DOF for serial chains. Initial conditions satisfying (9) allow the shaped dynamics of an n-DOF robot to project onto the dynamics of the corresponding $(n - k)$-DOF subrobot. This subsystem is entirely decoupled from the first k coordinates and thus behaves and can be controlled as a typical $(n-k)$-DOF robot. Moreover, the first k DOF evolve in a controlled manner according to momentum constraint (9). These coordinates converge to set-points or periodic orbits based on the subsystem trajectories and our choice of functional momentum maps $\lambda(q_j) = -\alpha_j(q_j - \tilde{q}_j)$, where α_j is a gain and $\tilde{q}_j$ is a desired angle, for $j \in \{1, k\}$.

We now present the application of reduction-based control to bipedal walking robots with branching structure.

V. Bipedal Walking Robots

A bipedal robot can be modeled as a hybrid system, which contains both continuous and discrete dynamics. We assume full actuation at the stance ankle of flat feet, which have

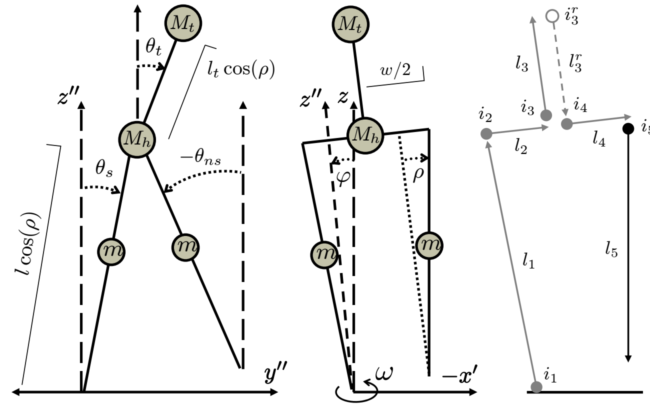

Fig. 2. The sagittal and frontal planes of a 3-D bipedal torso robot, along with its serial-chain mapping. Note that i_2 is a fixed angle interconnection.

instantaneous and perfectly plastic impact events. During the continuous swing phase, the contact between stance foot and ground is assumed flat without slipping. Note that some of these assumptions can be relaxed as in [16], [17]. We begin with some formalisms for hybrid systems from [3], [21].

Hybrid Systems. We describe simple hybrid systems with one continuous phase as "systems with impulse effects" [21].

Definition 4: A *hybrid control system* has the form

$$\mathscr{HC} : \begin{cases} \dot{x} = f(x) + g(x)u & x \in D \backslash G \\ x^+ = \Delta(x^-) & x^- \in G \end{cases},$$

where $G \subset D$ is called the *guard* and $\Delta : G \to D$ is the *reset map*. In our context, state $x = (q^T, \dot{q}^T)^T$ is in domain $D \subseteq TQ$ and input u in control space $U \subset \mathbb{R}^n$. A *hybrid system* $\mathscr{H}$ has no explicit input u (e.g., a closed-loop system), and a *hybrid flow* is a solution to a hybrid system.

We also must define periodicity, since bipedal walking gaits typically correspond to 2-step periodic solutions of hybrid systems due to side-to-side swaying motion. Letting $x(t)$ be a hybrid flow of $\mathscr{H}$, it is k-periodic if $x(t) = x(t + \sum_{i=1}^k T_i)$, for all $t \geq 0$, where T_i is the fixed *time to impact* between the $(i-1)^{th}$ and i^{th} discrete events [21]. Then, $x(t)$ is associated with its *k-periodic hybrid orbit* $\mathcal{O} = \{x(t) | t \geq 0\} \subset D$.

Stability of periodic hybrid orbits (i.e., limit cycles) is determined with the *Poincaré map* $P : G \to G$, which represents $\mathscr{H}$ as a discrete system between intersections with G (e.g., impact events). In particular, the k-composition of this map sends state $x_j \in G$ ahead k impact events by the discrete system $x_{j+k} = P^k(x_j)$. Thus, an k-periodic hybrid orbit $\mathcal{O}$ has an *k-fixed point* $x^* \in G \cap \mathcal{O}$ such that $x^* = P^k(x^*)$. We can numerically approximate the linearized map δP^k about x^*, by which we find the eigenvalues to determine local exponential stability (LES) of the discrete system [7].

Five-DOF Torso Biped Model. We now construct the model of a 5-DOF bipedal robot with a hip, splayed legs, and a torso (Fig. 2). Although this is a 3-D extension of the 2-D compass-gait-with-torso biped, the 3-D biped does not have stable passive walking gaits down slopes. Moreover, this model is entirely controlled-reducible, i.e., the irreducible tree structure is the last DOF, so we can use reduction-based control to construct pseudo-passive 3-D walking gaits from the sagittal plane. This model's hybrid control system is

$$\mathscr{HC}_{5\mathrm{D}}: \begin{cases} \dot{x} = f_{5\mathrm{D}}(x) + g_{5\mathrm{D}}(x)u & x \in D_{5\mathrm{D}} \backslash G_{5\mathrm{D}} \\ x^+ = \Delta_{5\mathrm{D}}(x^-) & x^- \in G_{5\mathrm{D}} \end{cases}.$$

We represent the configuration space of the 5-DOF biped by $Q_{5\mathrm{D}} = \mathbb{T}^2 \times \mathbb{T}^3$ with coordinates $q = (\omega, \varphi, \theta^T)^T$, where ω is the yaw (or heading), φ is the roll (or lean) from vertical, and $\theta = (\theta_{\mathrm{s}}, \theta_{\mathrm{t}}, \theta_{\mathrm{ns}})^T$ is the vector of sagittal-plane (pitch) variables as in the 2-D model. All other parameters, including leg splay angle ρ, are held constant.

We derive the continuous dynamics for $\mathscr{HC}_{5\mathrm{D}}$ using the previously described method. We start with Lagrangian

$$L_{5\mathrm{D}}(q, \dot{q}) = \frac{1}{2}\dot{q}^T M_{5\mathrm{D}}(q)\dot{q} - V_{5\mathrm{D}}(q),$$

with recursively-cyclic 5×5 inertia matrix[2]

$$M_{5\mathrm{D}}(\varphi, \theta) = \begin{pmatrix} m_\omega(\varphi, \theta) & \text{---} & M_{\omega,\varphi,\theta}(\varphi, \theta) \\ | & m_\varphi(\theta) & M_{\varphi,\theta}(\theta) \\ M^T_{\omega,\varphi,\theta}(\varphi, \theta) & M^T_{\varphi,\theta}(\theta) & M_\theta(\theta) \end{pmatrix}$$

and potential energy

$$V_{5\mathrm{D}}(\varphi, \theta) = -\frac{g}{2}(2m + M_h + M_t)(w - 2l\sin(\rho))\sin(\varphi) + V_\theta(\theta)\cos(\varphi), \quad (11)$$

which contains the planar subsystem potential energy

$$V_\theta(\theta) = \frac{g}{2}(l\cos(\rho)((3m + 2(M_h + M_t))\cos(\theta_s) - m\cos(\theta_{ns})) + 2l_t M_t \cos(\theta_t)). \quad (12)$$

The equations of motion for the fully actuated biped are then

$$M_{5\mathrm{D}}(q)\ddot{q} + C_{5\mathrm{D}}(q, \dot{q})\dot{q} + N_{5\mathrm{D}}(q) = B_{5\mathrm{D}}u, \quad (13)$$

where $C_{5\mathrm{D}}$ and $N_{5\mathrm{D}}$ are defined as usual and $B_{5\mathrm{D}}$ is invertible. These equations are associated with the control system $(f_{5\mathrm{D}}, g_{5\mathrm{D}})$ with input u. We model actuator saturation at torque constant U_{max}, so the control space is

$$U_{5\mathrm{D}} = \{u \in \mathbb{R}^5 : |u_i| \leq U_{max}, \forall i \in \{1, 5\}\}.$$

In order to model walking on a flat surface, we represent the swing foot height with unilateral constraint function

$$H_{5\mathrm{D}}(q) = l\cos(\rho)(\cos(\theta_s) - \cos(\theta_{ns}))\cos(\varphi) - (w - 2l\sin(\rho))\sin(\varphi).$$

States $x = (q^T, \dot{q}^T)^T$ corresponding to feasible walking are in domain $D_{5\mathrm{D}}$, the subset of $TQ_{5\mathrm{D}}$ where this height is nonnegative. Impact events are triggered by intersections with guard $G_{5\mathrm{D}} \subset D_{5\mathrm{D}}$, where the height of the swing foot is zero and decreasing (to exclude scuffing events):

$$G_{5\mathrm{D}} = \left\{ x \in D_{5\mathrm{D}} \ : \ H_{5\mathrm{D}}(q) = 0, \left(\frac{\partial H_{5\mathrm{D}}(q)}{\partial q}\right)^T \dot{q} < 0 \right\}.$$

[2]Detailed terms are provided on the author's homepage.

Following the method of [21], we compute the reset map[3]

$$\Delta_{5\mathrm{D}}(q, \dot{q}) = \begin{pmatrix} \Gamma_{5D} q \\ \Omega_{5D}(q)\dot{q} \end{pmatrix}, \text{ where } \Omega_{5D}(q) \in \mathbb{R}^{5\times 5},$$

$$\Gamma_{5D} = \begin{pmatrix} I_{2\times 2} & 0_{2\times 3} \\ 0_{3\times 2} & \Gamma_\theta \end{pmatrix} \text{ and } \Gamma_\theta = \begin{pmatrix} 0 & 0 & 1 \\ 0 & 1 & 0 \\ 1 & 0 & 0 \end{pmatrix}.$$

The signs of w and ρ are flipped at impact to model the change in stance leg.[4] We now construct a reduction-based control law for this torso robot.

VI. Reduction-Based Control Law

The control law is designed to recursively break cyclic symmetries in the special almost-cyclic manner. The inner loop of the controller shapes our robot's energy to the 2-almost-cyclic form, and the nested outer loop plays two roles:

1) Implements passivity-based control on the 2-D-subsystem to construct known planar flat-ground gaits.
2) Stabilizes to a surface defined by constraint (9) so that Theorem 1 holds.

This builds upon the construction of the single-stage controller of [3]. We ignore actuator saturation during this derivation, but simulations will demonstrate robustness.

Lagrangian Shaping Control. This controller shapes $L_{5\mathrm{D}}$ into a 2-ACL for controlled reduction to the biped's planar subsystem. Given configuration vector $q = (\omega, \varphi, \theta^T)^T$, the 5-DOF potential (11) is not cyclic in the lean variable φ, so we must impose a "controlled symmetry" with respect to this coordinate's rotation group $\mathbb{S}^1$. This is most naturally accomplished with potential shaping to replace $V_{5\mathrm{D}}$ with V_θ of (12), the planar walker's cyclic potential energy (constructed from a scaled height due to splay angle ρ). We will incorporate this shaping into the control law.

We begin with 2-ACL (4a) for $j = 1$, $k = 2$, $n = 5$:

$$L_{\lambda_1^2}(q, \dot{q}) = \frac{1}{2}\dot{q}^T M_{\lambda_1^2}(q_2^5)\dot{q} - W_{\lambda_1^2}(q, \dot{q}_2^5) - V_{\lambda_1^2}(q),$$

where $M_{\lambda_1^2}$, $W_{\lambda_1^2}$ and $V_{\lambda_1^2}$ are defined by substituting $M_{5\mathrm{D}}$ for M and V_θ for V_{fct} in (5)-(6). Direct calculation shows that the stage-2 functional Routhian associated with 2-ACL $L_{\lambda_1^2}$ is the Lagrangian of the scaled planar walker:

$$L_\theta(\theta, \dot{\theta}) = \tfrac{1}{2}\dot{\theta}^T M_\theta(\theta)\dot{\theta} + V_\theta(\theta),$$

which yields the reduced control system (f_θ, g_θ) with subsystem input v_θ.

Given this target reduction, we shape $L_{5\mathrm{D}}$ into $L_{\lambda_1^2}$ with

$$u = B_{5\mathrm{D}}^{-1}(C_{5\mathrm{D}}(q, \dot{q})\dot{q} + N_{5\mathrm{D}}(q) + M_{5\mathrm{D}}(q_2^5)M_{\lambda_1^2}(q_2^5)^{-1}(-C_{\lambda_1^2}(q, \dot{q})\dot{q} - N_{\lambda_1^2}(q) + B_{5\mathrm{D}}v)), \quad (14)$$

where $C_{\lambda_1^2}$ and $N_{\lambda_1^2} = \frac{\partial}{\partial q}V_{\lambda_1^2}$ are shaped as in (7), and vector $v = (v_\omega, v_\varphi, v_\theta^T)^T$ contains the auxiliary control inputs to be defined. Finally, using momentum map functions

[3]The velocity map's complexity prevents symbolic expression.

[4]Technically the hybrid model should then have two sets of continuous/discrete phases, but we forgo this caveat for simplicity and note that the system should be 2-periodic.

$\lambda_1(\omega) = -\alpha_1(\omega - \bar{\omega})$ and $\lambda_2(\varphi) = -\alpha_2\varphi$, for $\alpha_1, \alpha_2 > 0$, we establish heading control to constant angle $\bar{\omega}$ for the yaw DOF and correction to vertical for the roll/lean DOF.

Inputting (14) into $(f_{5\mathrm{D}}, g_{5\mathrm{D}})$, the shaped dynamics are

$$M_{\lambda_1^2}(q_2^5)\ddot{q} + C_{\lambda_1^2}(q, \dot{q})\dot{q} + N_{\lambda_1^2}(q) = B_{5\mathrm{D}}v.$$

We associate this with the new control system $(f_{\lambda_1^2}, g_{\lambda_1^2})$ with control input v to be defined next.

Subsystem Passivity-Based Control. Since we can decouple the robot's last three coordinates (the reduced subsystem), we can control it as a planar 3-DOF biped with well-known passivity-based techniques in v_θ. In particular, we employ slope-changing "controlled symmetries," a method that uses control to impose symmetries on the system dynamics with respect to ground orientation. This will allow our biped to walk on flat ground given the existence of planar walking cycles down shallow slopes [20].

Just as the planar compass-gait biped has known passive limit cycles down shallow slopes, so does the compass-gait-with-torso biped. However, a PD control law is needed to upright the torso, which behaves as an unstable inverted pendulum, during otherwise passive walking gaits [11]. We want to implement controlled symmetries on our 5-DOF biped's planar subsystem to harness these known gaits on flat ground. Therefore, we adopt a subsystem controller that both uprights the torso and maps passive gaits [20]:

$$v_\theta = B_\theta^{-1}\left(\frac{\partial}{\partial\theta}\left(V_\theta(\theta) - V_\theta(\theta+\beta)\right) + (0, v_{pd}, 0)^T\right) \quad (15)$$

where $v_{pd} = -k_p(\theta_t + \beta) - k_d\dot{\theta}_t$ and $\beta = 0.052$ rad, the slope angle yielding the desired passive limit cycle.

This subsystem control law is incorporated into the full-order shaped system $(f_{\lambda_1^2}, g_{\lambda_1^2})$ by defining the new control system $(\hat{f}_{\lambda_1^2}, \hat{g}_{\lambda_1^2})$ with input $v_1^2 = (v_\omega, v_\varphi)^T$ as in (8). Similarly, the 2-reduced, v_θ-controlled vector field $\hat{f}_\theta$ is defined as in (10). In order to ensure the decoupling of $\hat{f}_\theta$, we now design control law v_1^2 to enforce constraint (9).

Zero Dynamics Control. The beneficial implications of Theorem 1 only hold from the set of states satisfying (9), so we must use control outside of this set to exploit this result. We extend the approach of [2] in using output linearization to force trajectories toward these desired constraints. We first define output functions quantifying the error between actual and desired velocities according to (9):

$$h_i(q_i^5, \dot{q}_i^5) := \dot{q}_i - \frac{1}{m_{q_i}(q_{i+1}^5)}\left(\lambda_i(q_i) - M_{q_i, q_{i+1}^5}(q_{i+1}^5)\dot{q}_{i+1}^5\right)$$

for $i \in \{1, 2\}$. We use a control law that will zero these output functions in our MIMO nonlinear control system. In other words, we want to stabilize the "zero dynamics" surface

$$\mathcal{Z} = \left\{ \begin{pmatrix} q \\ \dot{q} \end{pmatrix} \in TQ : h_i(q_i^5, \dot{q}_i^5) = 0, \ \ \forall i \in \{1, 2\} \right\}.$$

This law is proportional in nature, parameterized by gains ξ_i, and depends on Lie derivatives of h_i with respect to vector fields $(\hat{f}_{\lambda_1^2}, \hat{g}_{\lambda_1^2})$, but we leave the details to [10]. Note that $v_1^2\big|_{\mathcal{Z}} = 0$, so this law does not interfere with Theorem 1.

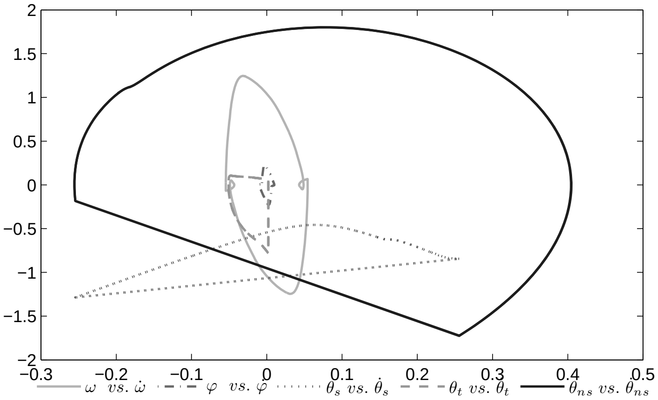

Fig. 3. Phase portrait of *straight-ahead* 2-periodic hybrid orbit $\mathcal{O}_{5\mathrm{D}}^{\mathrm{st}}$.

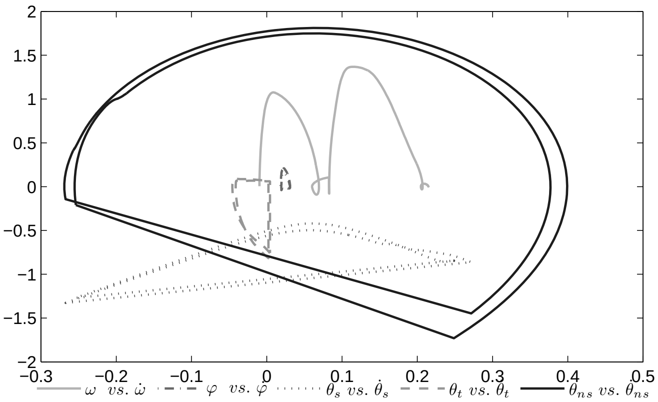

Fig. 4. Phase portrait of *turning* 2-periodic hybrid orbit $\mathcal{O}_{5\mathrm{D}}^{\mathrm{tu}}$.

VII. Simulations and Conclusions

After applying feedback control law (14) under actuator saturation, hybrid control system $\mathscr{HC}_{5\mathrm{D}}$ yields the autonomous closed-loop hybrid system $\mathscr{H}_{5\mathrm{D}}^{\mathrm{cl}}$, with physical and control parameters (16)-(17). Generally speaking, we cannot analyze the stability of $\mathscr{H}_{5\mathrm{D}}^{\mathrm{cl}}$ using the restricted Poincaré map associated with the reduced subsystem. At every impact event, joint velocities encounter a discontinuous jump off the conserved quantity surface $\mathcal{Z}$ (see [2] for an opposing special case). During the brief portion of each step cycle when zero dynamics law v_1^2 corrects this error, the solutions of $\hat{f}_{\lambda_1^2}$ and $\hat{f}_\theta$ cannot be analytically related by Theorem 1. We will show, however, that $\mathscr{H}_{5\mathrm{D}}^{\mathrm{cl}}$ is robust to these brief errors by considering the full-order behavior of the biped.

When walking straight-ahead on flat ground, $\mathscr{H}_{5\mathrm{D}}^{\mathrm{cl}}$ produces a 2-step periodic orbit, $\mathcal{O}_{5\mathrm{D}}^{\mathrm{st}}$ of Fig. 3, which is constructed from its planar subsystem's limit cycle. The intersection between $\mathcal{O}_{5\mathrm{D}}^{\mathrm{st}}$ and Poincaré section $G_{5\mathrm{D}}$ is the 2-fixed point (18). From this we numerically calculate the eigenvalue magnitudes (19) of the linearized Poincaré map over two steps. All magnitudes are within the unit circle, thus confirming local exponential stability. We also see that the yaw and lean dynamics follow 2-periodic orbits, a natural result of controlled reduction and our momentum functions.

$$\text{Physical parameters} \quad : \quad M_t = 10 \text{ kg}, \; l_t = 0.5 \text{ m}, \; M_h = 10 \text{ kg}, \; w = 0.1 \text{ m}, \; m = 5 \text{ kg}, \; l = 1 \text{ m}, \; \rho = 0.0188 \text{ rad} \tag{16}$$

$$\text{Control parameters} \quad : \quad \alpha_1 = 20, \; \bar{\omega} = 0, \; \alpha_2 = 30, \; \xi_1 = 30, \; \xi_2 = 15, \; k_p = 700, \; k_d = 200, \; \beta = 0.052 \text{ rad}, \; U_{max} = 30 \text{ Nm} \tag{17}$$

$$x^{*\mathrm{st}} \approx (0.0544, 0.0062, -0.2543, 0.0021, 0.2558, 0.0673, -0.0173, -1.2871, 0.0673, -1.7233)^T \tag{18}$$

$$\text{abs}(\{\text{eig}_i(x^{*\mathrm{st}})\}) \approx \{0.7629, 0.7629, 0.2745, 0.0736, 0.0344, 0.0134, 0.0034, 0.0003, 0.0003, 0.0000\} \tag{19}$$

$$x^{*\mathrm{tu}} \approx (0.2147, 0.0185, -0.2534, 0.0043, 0.2488, 0.0015, -0.0052, -1.2706, 0.0601, -1.7303)^T \tag{20}$$

$$\text{abs}(\{\text{eig}_i(x^{*\mathrm{tu}})\}) \approx \{0.7835, 0.3594, 0.2111, 0.2111, 0.0386, 0.0047, 0.0047, 0.0003, 0.0001, 0.0000\} \tag{21}$$

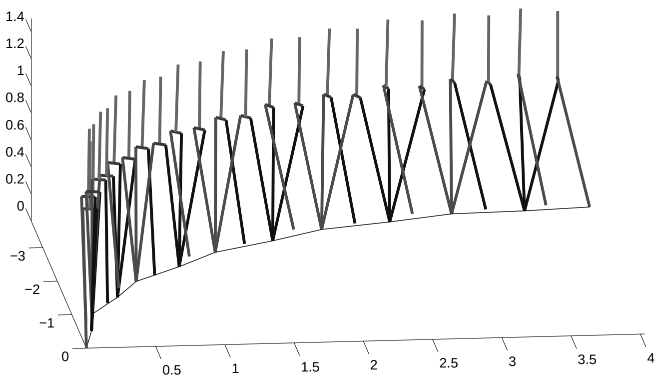

Fig. 5. A 90°-turn maneuver for the 5-DOF torso biped.

We demonstrate the steering capabilities of the biped with a 90° turn over several steps (Fig. 5). Starting with $\bar{\omega} = 0$, we increment this desired yaw angle by $\Delta\bar{\omega} = \pi/14$ every other step until $\bar{\omega} = \pi/2$. Once the biped meets this heading, its gait stably converges to the straight-ahead limit cycle of $\mathcal{O}_{5\mathrm{D}}^{\mathrm{st}}$ with a horizontally-shifted yaw orbit.

If we instead continue this constant-curvature steering, we observe convergence to a periodic turning gait modulo heading change. The 2-fixed point (20) with orbit $\mathcal{O}_{5\mathrm{D}}^{\mathrm{tu}}$ is confirmed LES (modulo $\Delta\bar{\omega}$) with eigenvalues (21). We see in Fig. 4 that $\mathcal{O}_{5\mathrm{D}}^{\mathrm{tu}}$ has a perturbed subsystem orbit compared to $\mathcal{O}_{5\mathrm{D}}^{\mathrm{st}}$, since the external leg takes longer strides (0.5361 m) than the inner leg (0.5008 m) along this curved path. This behavior occurs naturally (we have no reference trajectories) and resembles the human studies of [6]. In general, we find that stable turning gaits exist for a wide range of steering angles, as documented in [8], [9] for hipless bipeds.

We have shown that increasingly complex bipedal robots can achieve stable directional 3-D walking with reduction-based control. Our method embraces the beneficial passive dynamics of the robot in order to produce time-invariant and asymptotically stable walking with human-like swaying motion. This provides robustness to small perturbations (e.g., steering), naturally resulting in multiple types of dynamic walking gaits. Finally, these straight-ahead and turning gaits form a set of motion primitives for planning stable walking paths, which is the subject of current work in [8].

Acknowledgments

The authors thank Aaron D. Ames for his pioneering work on controlled reduction, Eric Wendel for the original simulation code, and the support of NSF Grant CMS-0510119.

REFERENCES

[1] D. Agahi and K. Kreutz-Delgado, "A star-topology dynamic model for multipedal locomotion," in *Conference on Decision and Control*, San Diego, CA, 1997.

[2] A. D. Ames and R. D. Gregg, "Stably extending two-dimensional bipedal walking to three dimensions," in *American Control Conference*, New York, NY, 2007.

[3] A. D. Ames, R. D. Gregg, and M. W. Spong, "A geometric approach to three-dimensional hipped bipedal robotic walking," in *Conference on Decision and Control*, New Orleans, LA, 2007.

[4] C. Chevallereau, J. W. Grizzle, and C. Shih, "Asymptotically stable walking of a five-link underactuated 3D bipedal robot," *IEEE Transactions on Robotics*, vol. 25, no. 1, pp. 37–50, 2008.

[5] S. H. Collins, M. Wisse, and A. Ruina, "A 3-D passive dynamic walking robot with two legs and knees," *Int. J. of Robotics Res.*, vol. 20, pp. 607–615, 2001.

[6] G. Courtine and M. Schieppati, "Human walking along a curved path. I. body trajectory, segment orientation and the effect of vision," *European Journal of Neuroscience*, vol. 18, no. 1, pp. 177–190, 2003.

[7] A. Goswami, B. Thuilot, and B. Espiau, "Compass-like biped robot part I: Stability and bifurcation of passive gaits," Institut National de Recherche en Informatique et en Automatique, Tech. Rep. 2996, 1996.

[8] R. D. Gregg, T. W. Bretl, and M. W. Spong, "Asymptotically stable gait primitives for planning dynamic bipedal locomotion in three dimensions," in *International Conference on Robotics and Automation*, Anchorage, AK, 2010, submitted.

[9] R. D. Gregg and M. W. Spong, "Bringing the compass-gait bipedal walker to three dimensions," in *International Conference on Intelligent Robots and Systems*, St. Louis, MO, 2009, to appear.

[10] ——, "Reduction-based control of three-dimensional bipedal walking robots," *Int. J. of Robotics Res.*, 2009, pre-print.

[11] J. K. Holm, D. Lee, and M. W. Spong, "Time-scaling trajectories of passive-dynamic bipedal robots," in *IEEE International Conference on Robotics and Automation*, Roma, Italy, 2007.

[12] A. D. Kuo, "Stabilization of lateral motion in passive dynamic walking," *Int. J. of Robotics Res.*, vol. 18, no. 9, pp. 917–930, 1999.

[13] J. E. Marsden and T. S. Ratiu, *Introduction to Mechanics and Symmetry*, 2nd ed. New York, NY: Springer, 2002.

[14] T. McGeer, "Passive dynamic walking," *Int. J. of Robotics Res.*, vol. 9, no. 2, pp. 62–82, 1990.

[15] R. M. Murray, Z. Li, and S. S. Sastry, *A Mathematical Introduction to Robotic Manipulation*. CRC Press, 1994.

[16] C. Shih, J. W. Grizzle, and C. Chevallereau, "Asymptotically stable walking and steering of a 3D bipedal robot with passive point feet," *IEEE Transactions on Robotics*, 2009, submitted.

[17] R. Sinnet and A. D. Ames, "3D bipedal walking with knees and feet: A hybrid geometric approach," in *Conference on Decision and Control*, Shanghai, China, 2009, to appear.

[18] M. W. Spong, "Passivity based control of the compass gait biped," in *IFAC World Congress*, Beijing, China, 1999.

[19] ——, "The passivity paradigm in bipedal locomotion," in *International Conference on Climbing and Walking Robots*, Madrid, Spain, 2004.

[20] M. W. Spong and F. Bullo, "Controlled symmetries and passive walking," *IEEE Transactions on Automatic Control*, vol. 50, no. 7, pp. 1025–1031, 2005.

[21] E. R. Westervelt, J. W. Grizzle, C. Chevallereau, J. H. Choi, and B. Morris, *Feedback Control of Dynamic Bipedal Robot Locomotion*. New York, New York: CRC Press, 2007.

[22] J. Wittenburg, *Dynamics of Multibody Systems*, 2nd ed. New York, NY: Springer, 2007.